https://doi.org/10.5194/nhess-2020-145
Preprint. Discussion started: 15 May 2020

Natural Hazards and Earth System Sciences Discussions

A classification scheme to determine wildfires from the satellite record in the cool grasslands of southern Canada: considerations for fire occurrence modelling and warning criteria

Dan K. Thompson[1], Kimberly Morrison[1]

[1]Canadian Forest Service, Northern Forestry Centre, Natural Resources Canada, Edmonton, Canada

Correspondence to: Dan K. Thompson (Daniel.Thompson@canada.ca)

Abstract. Daily polar orbiting satellite thermal detections since 2002 were used as the baseline for quantifying wildfire activity in the mixed grass and agricultural lands of southernmost central Canada. This satellite thermal detection record includes both the responsible use of fire (e.g. for clearing crop residues, grassland ecosystem management, and traditional burning), as well as wildfires in grasslands and agricultural lands that pose a risk to communities and other values. A database of known wildfire evacuations and fires otherwise requiring suppression assistance from provincial forest fire agencies was used to train a model that classified satellite fire detections based on weather, seasonality, and other environmental conditions. A separate dataset of high-resolution (LANDSAT 8 thermal anomalies) of responsible agricultural fire use (e.g. crop residue burning) was collected and used to train the classification model to the converse. Key common attributes of wildfires in the region included occurrence on or before the first week of May with high rates of grass curing, wind speeds over 21 km h^{-1}, relative humidity values typically below 40% and fires that are detected in the mid-afternoon or evening. Overall, grassland wildfire is found to be restricted to a small number of days per year, allowing for the future development of public awareness and warning systems targeted to the identified subset of weather and phenological conditions.

1 Introduction

Wildfire is a widespread and commonplace phenomenon in Canada, with contexts ranging from an integral component of traditional land use (Lewis et al., 2018), a purely natural disturbance (i.e. lightning ignition) process with little human impact (Whitman et al., 2018), to a devastating natural hazard to communities (Christianson et al., 2019). Fire (both human and natural ignition) is most common in Canada in its interior, west of the Great Lakes and east of the Rocky Mountains, where a belt of high fire frequency extends from the subarctic forests of the Deh Cho (Mackenzie Valley) through to the drier southern boreal forest-grassland transition (Boulanger et al., 2014). Within this broad north-south transect, the density of values at risk varies greatly, from sparse communities in the northern forest with limited industrial activities to a dense matrix of industry with dispersed agriculture and rural habitation (Johnston and Flannigan, 2018). At the southern limit of the boreal forest in western Canada, climatic limitations to widespread forests created a natural ecotone towards a more open deciduous forest and grass parkland (Hogg, 1994; Zoltai, 1975), which has been almost entirely converted to intensive agriculture with a steady rate

https://doi.org/10.5194/nhess-2020-145
Preprint. Discussion started: 15 May 2020


Natural Hazards and Earth System Sciences Discussions

of increasing agricultural conversion (Hobson et al., 2002). This is in contrast to the United States, where extensive natural grasslands intermix with dry conifer forests in areas of greater wildfire occurrence (Gartner et al., 2012). In Canada, at the southern forest limit and further south, the wildland-urban interface transitions to widespread human agriculture and only patches of broadleaf (deciduous) aspen forest (Hogg, 1994). Though smaller, localized grasslands in a larger matrix of forest are readily integrated into local wildfire likelihood assessments (Parisien et al., 2013), large-scale assessments of wildfire likelihood are often based on modelling that utilizes forest fire management agency records (Parisien et al., 2013; Stockdale et al., 2019), and therefore exclude wildfires in agricultural areas where no such land management agency records exist. In this primarily agricultural region, controlled agricultural burning is commonly used to burn off excess crop residue (Chen et al., 2005). The use of a purely thermal remote sensing approach to determine the risk of wildfire (Rogers et al., 2015) (i.e. fires being actively suppressed but not under control) can count responsible fire use in agriculture as wildfire occurrence.

In Canada, both forest fire and grass fire likelihood and spread are predicted using a common system, the Canadian Forest Fire Danger Rating System (CFFDRS), developed and maintained by the Canadian Forest Service starting in the 1930s. The system allows for the prediction of grass fire rate of spread (metres/minute), fire intensity (equivalent to flame height), and expected growth rate (fire size over time). Fire weather is quantified using daily temperature, humidity, and wind speed, with grass curing (the ratio of dead grass to live grass) being a critical variable that controls grass fire behaviour. Under the Canadian Fire Weather Index System (Van Wagner, 1987), the fire danger classes for public awareness (i.e., Low, High, Extreme, etc.) are based on a scaling of the expected head fire intensity of an idealized pine stand with a pine needle surface fuel bed. In this type of forest, wind speed, humidity, and drought will impact fire behaviour, but the lack of deciduous trees or understory vegetation negate seasonal phenology beyond needle flush. When this Fire Weather Index scheme is then applied across regions dominated by grasslands, agriculture, or deciduous tree or shrubs, the Fire Weather Index alone and associated Fire Danger classes need to be adjusted for leaf-on or greenup conditions (Alexander, 2010; Chéret and Denux, 2011).

Recent research in Australia has highlighted the importance of grass fuel loading as a negative influence on fire rate of spread, whereby a doubling of grass fuel load from the standard assumption of 0.35 kg of fuel m^{-2} to 0.70 kg m^{-2} results in a 10 % reduction in spread rate (Cruz et al., 2018). Conversely, a 50 % reduction in fuel load results in between a 10–30 % increase in spread rate; flame height (proportional to fireline intensity) increased to the power of 0.60 with increased fuel loading however, meaning a doubling of fuel loading results in a 50 % increase in flame height. Accordingly, under dry conditions, light agricultural residues may burn with high rates of spread though lower flame heights, while higher fuel loads in agricultural residues would likely burn slower but with substantially larger flames. In mixed forest and open grass-type fuel landscapes, the lower intensity of grass fires despite the higher spread rates typically results in higher rates of successful fire suppression for grasslands in empirical (Finney et al., 2009) and modelling (Reimer et al., 2019) studies compared to standing forest. Rapid fuel moisture gains during typical night-time periods results in limited nocturnal fire activity potential (Kidnie and Wotton, 2015) except during exceptional periods of sustained wind and very low humidity (Lindley et al., 2019).

https://doi.org/10.5194/nhess-2020-145
Preprint. Discussion started: 15 May 2020


Natural Hazards and Earth System Sciences Discussions

The overall goal of this study is to examine the differing environmental conditions most common during agricultural fires, and to contrast that with documented wildfires in the region. The first specific goal is to apply a classification model to historical fire thermal detections (2002–2018) in order to determine the relative densities of agricultural burning and smaller, mostly undocumented grassland wildfires. The second goal is to develop an initial data-driven wildfire occurrence criteria usable for public warning specific to grassland and agricultural regions of southern Canada.

2 Materials and Methods

2.1 Study Area

The study area encompasses the entire primary agriculture zone of central-western Canada (Prairies) as well as the forest-agriculture mix that extends north (to 58º N at its furthest point) and east to (as far as 96º W) where the shallow granitic soils of the Canadian Shield are found (Fig. 1). The southern limit of the study area is the United States border at 49º N, and the western limit is the continuous forest and protected areas of the Rocky Mountains. The climate of the region is cool and continental, with mean annual temperature ranging from 0.6º C in Peace River to 5.9º C at Lethbridge. The number of frost-free days is as few as 119 in Peace River, and as many as 132 in areas east of Lethbridge. Foehn winds (locally known as Chinooks) on the eastern side of the Rocky Mountains cause periodic temperature increases above freezing during winter, allowing for occasional winter grass fires. Snowmelt typically occurs in March-April in the southern extent, and April- early May further north. Annual precipitation varies from close to 600 mm in the easternmost edge of the study area near Winnipeg to as little as 316 mm in areas northeast of Lethbridge. Precipitation is heavily weighted to convective precipitation in the months of June-August. April and October are typically the two driest snow-free months.

Overall, 42 % of the study area is agricultural land or grasslands. Land ownership in the agricultural area is almost entirely privately held, with the exception of First Nations reserves (1.6 %), parks and protected areas (2.4 %), and provincial grazing reserves (1.8 %). Wildfire response is primarily volunteer-driven at the local community level (McGee et al., 2015). At the northern fringe of agriculture, private land is intermixed with provincially (sub-national) owned lands that are managed primarily for timber, and wildfire response is entirely the responsibility of provincial fire management agencies outside of settlement boundaries. Remotely-sensed land cover data at 30 m resolution (Agriculture and Agri-Food Canada, 2018) was used to distinguish forested areas from open fuels (including permanent croplands, pastures, native grasslands, and treeless wetlands) all of which share similar phenology and flammability. Broadleaf crops vs cereals were not distinguished.

2.2 Fire occurrence records

In the forest-agriculture mix, we used comprehensive fire history records from wildfire management agencies, as compiled in the Canadian National Fire Database (CNFDB) (Hanes et al., 2018). In the agricultural zone, the CNFDB provides only a

https://doi.org/10.5194/nhess-2020-145
Preprint. Discussion started: 15 May 2020


Natural Hazards and Earth System Sciences Discussions

95 partial sample of wildfires in the region, as larger fires that required a mutual aid response from provincial agencies are documented in the database, despite not being located in the provincial wildfire agencies area of responsibility. Additional reporting on wildfire occurrence in the agricultural zone is provided by the Canadian Wildfire Evacuation Database (Beverly and Bothwell, 2011), which since 2010 has collected information on wildfire evacuation in grassland areas in addition to forest fires dating back to the 1980s.

100

Records from fire management agencies and evacuations provide a partial sample of the true extent of wildfires in the agricultural zone, and capture completely the occurrence of wildfire in the provincial forest. Remotely-sensed thermal detection of active wildfire from the polar-orbiting NASA Aqua and Terra satellites that pass over Canada at 1300h local time were used as a spatially unbiased (but time-limited) sample of fire activity in the area. A standard MODIS collection from
105 2002-2018 (MOD14A1 and MYD14A1) (Giglio, 2015) with 1 km resolution was screened for persistent industrial heat sources and combined with a grid of daily Canadian Fire Weather Index system variables (Lee et al., 2002) to produce a database of fire thermal detections that spans both the responsible use of fire in land clearing and vegetation management, as well as out of control wildfire (Fig. 2). Thermal detections associated with fire agency records or evacuations (see supplementary materials for details) were set aside for later model creation and validation.

110

The responsible use of fire in the region includes traditional burning by First Nations, prescribed burning by fire management agencies to reduce fuel loads in grasslands (McGee et al., 2015), burning of crop residues (Chen et al., 2005), and pile burning during land clearing operations where residual tree biomass is burned during agricultural land conversion (Hobson et al., 2002). Other than prescribed burning, no official documentation exists for this type of fire use, and could otherwise be conflated with
115 wildfires as documented by remote sensing. In order to discriminate between responsible fire use and wildfires, we used the 30 m short-wave infrared thermal detections from the LANDSAT 8 satellite (Kato et al., 2018) in order to classify clusters of thermal detections as fire use if they correspond to geometric patterns associated with prescribed burning or other controlled fire (Fig. 3). A total of 41 LANDSAT hotspot clusters were manually classified in this manner; fire weather and landcover was associated with these detections similar to the MODIS detections. These LANDSAT detections are limited in spatial scale
120 as the satellite only returns over an area every two weeks, so these records are at best a small sample of the entire fire activity in the region (approximately 1/14, or 7 %), and only a sample of LANDSAT data was used in this study. All responsible use of fire is referred to as agricultural fire in this paper.

2.3 Satellite grass curing

125 Grass curing (the fraction of dead grass with moisture content controlled by atmospheric conditions) is the primary control on the fire spread potential in grass fuels, overriding all other factors (Cruz et al., 2015). However, capturing the complexities of plant phenology in the simple daily weather scheme used by the Fire Weather Index system or similar scheme is challenging

https://doi.org/10.5194/nhess-2020-145
Preprint. Discussion started: 15 May 2020


Natural Hazards and Earth System Sciences Discussions

(Jolly et al., 2005). For this retrospective analysis, we leverage satellite greenness as a proxy for grass curing, similar to (Pickell et al., 2017). In this study, we leverage historical 16-day composite NDVI (MOD13Q1 and MYD13Q1) (Didan et al., 2015) at 250 m resolution. A simple linear transform was used to convert between NDVI and percent curing:

$$P_{curing} = \frac{NDVI_t - \min(NDVI)}{\max(NDVI) - \min(NDVI)} \quad (1)$$

Where $NDVI_t$ is the measured NDVI at time *t*, *min(NDVI)* represents the per-pixel minimum snow-free NDVI value, and *max(NDVI)* is the per-pixel maximum NDVI climatology. Both the min and max values are based on the average of the annual maxima and minima from 2002 to 2014 (*i.e.* n = 12 per pixel for both min and max calculations).

All hotspot clusters with less than 40 % open fuels (grasslands, croplands, and treeless wetlands) were not considered grass fires and were eliminated from this study. It was noted that there were several hotspot clusters remaining near Fort McMurray, an area known not to have much grass. These clusters were also eliminated from this study, as they looked to be in a previously burned area dominated by shrubs, grass, and aspen, rather than a prairie grassland.

2.4 Classification of thermal detections

In total, 113 MODIS clusters (representing 576 total individual hotspots) were associated with documented wildfire, and 41 MODIS clusters, confirmed to be agricultural controlled burning via LANDSAT imagery, were classified as agriculture fire use. These data were then used to build models to classify the hotspot clusters as either agriculture fire or wildfire using Generalized Additive Models (GAM) as binomial models (binary of wildfire or not) were built using the R package *mcgv* (Wood, 2019), with splines used for variables with an expected non-linear response such as Day of Year, hour of detection, wind speed, and curing (Eq. (1)). This model was validated using leave-one-out cross validation. These GAMs account for multiple non-linear responses but not interactions between predictors. Alternately, regression trees were constructed using the *rpart* package (Therneau et al., 2019) to classify wildfires from thermal detections using a simple conditional threshold-type model. Percent grass curing was not used in the model, as it is highly site-specific compared to the weather variables that vary only regionally on a given day. As a result, only wildfires and agricultural fires with moderate to high curing (>40 %) were used to build the regression tree.

3. Results

Environmental, remotely sensed, and weather variables related to the distribution of agricultural vs wildfires are shown in Fig. 4. Both fire types (agricultural vs wildfires) show a strong peak in the spring period after snow melt (Day of Year, Fig. 4a), centred on late April and early May, with a slightly earlier peak for wildfires. The curing fraction of the grass or agricultural residue is lower for wildfires compared to agricultural fires (Fig. 4b), which may be due to NDVI artifacts from tillage (Zhang

https://doi.org/10.5194/nhess-2020-145
Preprint. Discussion started: 15 May 2020


Natural Hazards and Earth System Sciences Discussions

et al., 2018). The hour of first detection (Fig. 4c) is largely limited by the 1300h local time overpass at nadir for MODIS. Night-time fire detections at the (0100 h) local 1am overpass are rare even for the wildfires. Pre-fire drying conditions as parameterized in the Fire Weather Index (Duff Moisture Code (DMC) and Drought Code (DC)) show much larger right skews for wildfires. In the case of the DMC (Fig. 4d), which represents the moisture content of the forest floor beyond 2 cm depth, 26% of the wildfire data have DMC values beyond the maximum DMC for agricultural burning of 67 (approx. 17 days without rain exceeding 1.5 mm). DC (Fig. 4e) shows a similar trend: 5% of agricultural fires have a DC of 470 or greater compared to 27% of wildfires. Observed fire weather values (noon local standard time measurements of surface weather on the day of first fire detection) showed a meaningfully larger number of wildfires when relative humidity (Fig. 4f) was below 20 %, more agricultural fires when noon air temperatures are below 10°C (Fig. 4g), and far more wildfires when noon 10-m wind speeds exceed 25 km h^{-1} (Fig. 4h). The noon temperature, relative humidity, and wind speed form the basis of the calculation of the Fine Fuel Moisture Code (Fig. 4i) which shows a peak for agricultural burning at FFMC 90 versus 92 for wildfires. Finally, the natural logarithm of the Fire Radiative Power (FRP) of the MODIS detection (Fig. 4j) showed far more variance in wildfires compared to agricultural fires. No agricultural fires exceeded 400 MW in the sample of confirmed agricultural fires. The median number of thermal detection points per wildfire was 2 but as high as 55, in contrast with agricultural fires where the maximum number of thermal detections in a cluster is 6. Only 16 % of wildfires contained more than 6 hotspots in a cluster.

The above variables were assessed in a binomial generalized additive model, shown in Fig. 5. The GAM model was able to explain 68 % of the variance in the data, with strong non-linear predictors in Day of Year, curing, and wind speed. Hour of detection, relative humidity and DC were found to be significant in the GAM model as linear predictors, with odds ratios (increased rate of wildfire per integer increase in predictor value) of 1.32x per hour, 1.17x per unit decrease in RH, and 2.45x per hundred units of DC. Despite the lack of interactions between predictors in all GAM models, the model had a high overall predictive power when tested using a leave-one-out framework, with sensitivity of 82 % (true positive rate), specificity (true negative rate) of 87 %, an area under receiver operating characteristic curve (AUC) of 0.88, and a Critical Success Index of 0.78 (Table 1). The cutoff of the overall GAM model binomial output of 0.70 provided the optimal model performance.

A simple decision tree was constructed from the same dataset to look at simple threshold-based classification schemes. (Fig. 6). An Initial Spread Index (ISI) (proportional to the fire's rate of spread) was found to be the strongest predictor, with 92 % accuracy in predicting wildfires vs agricultural fires. Next, the Fine Fuel Moisture Code was also found to correctly classify 98 % of fire detections when wildfires are classified ISI >=15. For fires with ISI <15, high percent curing (*i.e.* low NDVI, indicative of plowed fields in the vicinity or recent adjacent agricultural burning) over 86 % was a strong indicator of controlled agricultural burning, with 84 % accuracy. In areas with lower NDVI/curing values, ISI values >= 11 (but under 15) were wildfires 90 % of the time, and lower ISI values showed no meaningful pattern, with 58 % being agricultural burns. Overall, the single threshold of ISI >= 15 appears to be the best balance between simplicity and accuracy, as it correctly identifies 82 % of all the fires with little commission of only one agricultural fire. The meteorological conditions resulting in an ISI >= 15

https://doi.org/10.5194/nhess-2020-145
Preprint. Discussion started: 15 May 2020


Natural Hazards and Earth System Sciences Discussions

are shown in Appendix A. Overall, this decision tree model had a lower AUC of 0.78 compared to the GAM, where as the decision tree had a higher True Positive Rate of 0.95 and a far lower True Negative Rate of 0.60 (Table 1). However, the Critical Success Index of 0.82 and overall Accuracy of 0.85 is slightly better than the GAM. A total of 11 wildfires in early May of 2009 occurred at reportedly low values of DC (<100). A DC of 100 is far below the minimum DC recorded for agricultural fires (which generally have DC that is lower that wildfires), and resulted in a terminal node of wildfires at a very low DC with no regard for ISI. This would lead to the false conclusion that all detections with a low (wet) DC are wildfires. These observations were not included in the decision tree. Therefore, the decision tree should be considered applicable when DCs exceed 100, a moisture condition range at which overwinter precipitation measurements can induce uncertainty into spring DC values (Chavardès et al., 2019).

In addition to the classification trees presented in Fig. 6, some properties of wildfires show meaningful extreme values beyond all agricultural fires values with or without meaningful differences to overall distribution (Fig. 4) or as a linear predictor in the GAM (Fig. 5). Median FRP between all agricultural burns (39 MW) and all wildfires (59 MW) are similar, and a non-parametric Mann-Whitney *U* test on the two samples did not differ significantly (Mann–Whitney $U = 1860$, $n_1 = 113$, $n_2 = 41$, $p < 0.44$ two-tailed). However, on the higher end of FRP, wildfires showed a much larger right skew to the FRP values, with the 99th percentile of agricultural fire FRP of 233 MW, while this corresponded to the 86th percentile of wildfire FRP (or the largest 14% of the wildfire data). With the maximum observed wildfire FRP being 1174 MW, this allows for an additional logical scheme to discriminate wildfires from agricultural burning not captured in the above decision tree, where MODIS hotspot FRP values > 233 MW can be confidently classified as wildfires. Similarly, median noon wind speeds between agricultural fires (15.5 km h^{-1}) and wildfires (21.2 km h^{-1}) were similar, though distributions differed significantly (Mann–Whitney $U = 1387$, $n_1 = 113$ $n_2 = 41$, $p = 0.0001$ two-tailed). Some 30% of wildfire wind speeds exceeded the 90th percentile of agricultural fire wind speeds (22 km h^{-1}), allowing for an additional simple classification consideration for fire thermal detections during periods of high wind speed.

When the GAM model is applied to the 24,316 hotspots clusters in the entire MODIS dataset, 30 % of hotspots were detected under conditions that are most similar to documented wildfires (Fig. 8), these have a strong regional gradient with more wildfires in the eastern portion of the study area. The seasonal and spatial patterns along lines of equal longitude are portrayed in a Hovmoller diagram in Fig. 9.

4. Discussion

The dataset used in this study purposely utilized the longer-duration MODIS dataset from 2002 onwards, rather than the shorter duration VIIRS dataset from 2012 onwards. Though both sensors are capable of fire detection in the midwave infrared, VIIRS is in theory capable of detecting smaller or less intense agricultural fires (Johnston et al., 2018; Zhang et al., 2017) which offers

https://doi.org/10.5194/nhess-2020-145
Preprint. Discussion started: 15 May 2020


Natural Hazards and Earth System Sciences Discussions

little advantage when the goal is the detection of larger wildfires in the region. Moreover, one of the goals of this study is to examine broad spatial trends in fire occurrence (Fig. 8), where a longer record is ideal. Recently launched geostationary weather-oriented earth observation platforms such as GOES, Meteosat, and Himawari offer many advantages for monitoring short-lived wildfires, with scan rates every 10–15 minutes (Hall et al., 2019). The northern latitude of the study area (49–59° N) causes a severe degradation of the pixel size of GOES geostationary fire detections to 4 km and limited FRP resolving capacity (Hall et al., 2019). The dataset and classification criteria presented here can assist in improving the confidence in real-time wildfire detection in these areas with widespread fire use on the landscape.

.

In all likelihood, many of these >7 500 wildfires identified over 17 years (or 441 fires per year over a 115 Mha study area) are smaller, briefly out of control fires where agricultural burning gets beyond direct suppression and burns over a number of adjacent agricultural fields until the wildfire encounters a roadway (typically over 10 m of fuel-free width), which readily stops most wildfires in grass and agricultural residue fuels (Cheney, and Sullivan, 2008). Given the generally widespread dispersed population density of the area, the vast majority of wildfires in the region are detected and reported by the public (McGee et al., 2015), such that satellites as the first mode of wildfire detection is of limited utility in the region, compared to more northerly and remote areas (Johnston et al., 2018). However, satellites provide a consistent technique for medium-resolution fire extent reporting and mapping that can prove useful for emergency managers (Lindley et al., 2019). Moreover, wildfire growth modelling (Sá et al., 2017) and smoke dispersion forecasts (Chen et al., 2019) require real-time analysis and forecasting initialized using remotely-sensed fire detections.

Grass dries much quicker than the forest floor, meaning the largest discrepancy between forest floor (FFMC) and open grass moisture content lies within 2–3 days after rainfall where grass is drier, after which the moisture content in the FFMC and a Grass Fuel Moisture Content model are similar (Kidnie and Wotton, 2015). In the decision tree model (Fig. 6), RH is not directly included, though FFMC values over 93 are found only during periods of low RH and multiple days since rainfall. This is in contrast with (Lindley et al., 2011) who found that RH thresholds below 25 % and particularly below 20 % are responsible for most grassland wildfires in west Texas. RH however is not an ideal proxy for fuel moisture across the wide range of air temperatures found in the region, as RH alone does not account for variable vapour pressure deficit at different temperatures (Srock et al., 2018). The interaction of temperature and vapour pressure is parameterized to some extent in the FFMC (Van Wagner, 1987).

The study region is often impacted by prolonged dry periods. The study region experienced profound drought in the 1999–2005 period (Hanesiak et al., 2011) that corresponds to the start of the study period. Drought itself was a minor first-order predictor of grassland wildfire in this dataset, as an increase of 100 DC units (DC is wettest at zero and reaches ~700 in late summer droughts) results in the odds of a wildfire over an agricultural fire increase by 2.45 times. In addition to the absolute value of the DC, drought itself in the grasslands and agricultural areas of North America results in significant reductions in

https://doi.org/10.5194/nhess-2020-145
Preprint. Discussion started: 15 May 2020


Natural Hazards and Earth System Sciences Discussions

NDVI (Gu et al., 2007) that therefore directly increases grass curing as estimated in this study (Eq. (1)) and hence the window of grassland wildfire susceptibility.

The thresholds at which agricultural fire detections are overtaken by wildfires occurs at fire intensity thresholds that correspond to the limits of ground-based wildfire suppression. Following the Canadian Forest Fire Danger Rating System (Forestry Canada, 1992) for an O-1a (matted grass) fuel type, Initial Spread Index values of 15 with grass curing between 75–80 % (Fig. 5), the resultant spread rate of 24 m min^{-1} (1.4 km h^{-1}) and intensity of approximately 2 500 kW m^{-1} (flames 2 m long) is near the upper limit of suppression, particularly when fire sizes exceed 2–3 ha (Hirsch et al., 1998).

Under climate change, the agricultural and grassland region of Canada is anticipated to move northward (Schneider et al., 2009), though this rate of transition will be dampened in peatland areas (Schneider et al., 2016) and those not disturbed by wildfire (Stralberg et al., 2018). Natural grasslands are expected to increase particularly in areas of rapidly accelerating fire occurrence, where younger forests disturbed by severe wildfire are prone to large increases in grass cover (Whitman et al., 2019). Moreover, a dense grass cover is problematic in recently planted forests north of the study region, as it can outcompete tree seedlings (Lieffers et al., 1993), and is likely to be exasperated by the expected lower overall canopy density (Lieffers and Stadt, 1994) brought about by a drier future climate (McDowell and Allen, 2015). Active conversion of forest to agricultural lands is likely to continue (Hobson et al., 2002), as is the natural expansion of grasslands on drier, south-facing slopes in the boreal forest where their range is currently limited to at high latitudes (Sanborn, 2010).

5. Conclusions

A classification scheme was developed to discriminate remotely sensed agricultural fires vs wildfires in the southern grasslands of continental Canada through an analysis of historical wildfires and documented agricultural fires. Effective schemes for discriminating fire types were produced using continuous data (Generalized Additive Models) as well as threshold-based classification trees. A combination of weather, vegetation condition, and temporal variables provided the best predictors. Initial Spread Index values exceeding 15 at noon on the day of the fire was the most powerful threshold for identifying wildfires, grass curing values between 60–85 % was the best non-linear spline predictor in the GAM. Fire Radiative Power was effective in discriminating wildfires only in the 14 % of wildfires with very high FRP values that exceeded the highest documented FRP in the agricultural fire dataset. Similar discrimination utility was seen in the Drought Code. Overall, the majority of the most power predictors of grassland wildfire stem from weather observations and remotely sensed metrics of the pre-fire environment, and are thus available for forecasting and real-time classification of satellite thermal detections. This work provides a foundation from which future public warning products can be derived.

https://doi.org/10.5194/nhess-2020-145
Preprint. Discussion started: 15 May 2020


Natural Hazards and Earth System Sciences Discussions

Author contributions: Conceptualization, DKT; Funding acquisition, DKT; Methodology, DKT and KM; Formal Analysis, DKT and KM; Data curation, KM; Investigation, KM; Project administration, DKT; Resources, DKT; Supervision, DKT; Validation, DKT and KM; Visualization, DKT and KM; Writing – original draft, DKT; Writing – review & editing, KM.

Funding: Funding for this project was provided by Crown Indigenous Relations and Northern Affairs Canada under the First Nations Adapt program.

Conflicts of Interest: The authors declare no conflicts of interest.

Acknowledgements: The authors would like to acknowledge Brett Moore and Chris Dallyn for providing valuable feedback on the manuscript and Peter Englefield for both feedback the acquisition of the MODIS hotspot and percent curing data.

References

Agriculture and Agri-Food Canada: Land Use 2010, [online] Available from: https://open.canada.ca/data/en/dataset/9e1efe92-e5a3-4f70-b313-68fb1283eadf (Accessed 9 March 2020), 2018.

Alexander, M. E.: Surface fire spread potential in trembling aspen during summer in the Boreal Forest Region of Canada, For. Chron., 86(2), 200–212, doi:10.5558/tfc86200-2, 2010.

Beverly, J. L. and Bothwell, P.: Wildfire evacuations in Canada 1980–2007, Nat. Hazards, 59(1), 571–596, doi:10.1007/s11069-011-9777-9, 2011.

Boulanger, Y., Gauthier, S. and Burton, P. J.: A refinement of models projecting future Canadian fire regimes using homogeneous fire regime zones, Can. J. For. Res., 44(4), 365–376, doi:10.1139/cjfr-2013-0372, 2014.

Chavardès, R. D., Daniels, L. D., Eskelson, B. N. I. and Pickell, P. D.: Monthly adaptations of the Drought Code reveal nuanced fire–drought associations in montane forests with a mixed-severity fire regime, Int. J. Wildland Fire, 28(6), 445–455, doi:10.1071/WF18119, 2019.

Chen, J., Anderson, K., Pavlovic, R., Moran, M. D., Englefield, P., Thompson, D. K., Munoz-Alpizar, R. and Landry, H.: The FireWork v2.0 air quality forecast system with biomass burning emissions from the Canadian Forest Fire Emissions Prediction System v2.03, Geosci. Model Dev., 12(7), 3283–3310, doi:https://doi.org/10.5194/gmd-12-3283-2019, 2019.

Chen, Y., Tessier, S., Cavers, C., Xu, X. and Monero, F.: A survey of crop residue burning practices in Manitoba, Appl. Eng. Agric., 21(3), 317–323, 2005.

Cheney, P. and Sullivan, A.: Grassfires: Fuel, Weather and Fire Behaviour, CSIRO Publishing, Clayton, Australia. [online] Available from: https://www.publish.csiro.au/book/5971 (Accessed 13 December 2019), 2008.

Chéret, V. and Denux, J.-P.: Analysis of MODIS NDVI Time Series to Calculate Indicators of Mediterranean Forest Fire Susceptibility, GIScience Remote Sens., 48(2), 171–194, doi:10.2747/1548-1603.48.2.171, 2011.

https://doi.org/10.5194/nhess-2020-145
Preprint. Discussion started: 15 May 2020

Christianson, A. C., McGee, T. K. and Whitefish Lake First Nation 459: Wildfire evacuation experiences of band members of Whitefish Lake First Nation 459, Alberta, Canada, Nat. Hazards, 98(1), 9–29, doi:10.1007/s11069-018-3556-9, 2019.

Cruz, M. G., Gould, J. S., Kidnie, S., Bessell, R., Nichols, D. and Slijepcevic, A.: Effects of curing on grassfires: II. Effect of grass senescence on the rate of fire spread, Int. J. Wildland Fire, 24(6), 838–848, doi:10.1071/WF14146, 2015.

Cruz, M. G., Sullivan, A. L., Gould, J. S., Hurley, R. J. and Plucinski, M. P.: Got to burn to learn: the effect of fuel load on grassland fire behaviour and its management implications, Int. J. Wildland Fire, 27(11), 727–741, doi:10.1071/WF18082, 2018.

Didan, K., Munoz, A. B., Solano, R. and Huete, A.: MODIS Vegetation Index User's Guide (MOD13 Series) Version 3.00, Vegetation Index and Phenology Lab, The University of Arizona. [online] Available from: https://vip.arizona.edu/documents/MODIS/MODIS_VI_UsersGuide_June_2015_C6.pdf, 2015.

Finney, M., Grenfell, I. C. and McHugh, C. W.: Modeling Containment of Large Wildfires Using Generalized Linear Mixed-Model Analysis, For. Sci., 55(3), 249–255, doi:10.1093/forestscience/55.3.249, 2009.

Forestry Canada: Development and structure of the Canadian Forest Fire Behavior Prediction System. [online] Available from: https://cfs.nrcan.gc.ca/publications?id=10068 (Accessed 28 October 2019), 1992.

Gartner, M. H., Veblen, T. T., Sherriff, R. L. and Schoennagel, T. L.: Proximity to grasslands influences fire frequency and sensitivity to climate variability in ponderosa pine forests of the Colorado Front Range, Int. J. Wildland Fire, 21(5), 562–571, doi:10.1071/WF10103, 2012.

Giglio, L.: MODIS Collection 6 Active Fire Product User's Guide Revision A, Department of Geographical Sciences, University of Maryland. [online] Available from: https://lpdaac.usgs.gov/documents/88/MOD14_User_Guide_v6.pdf, 2015.

Gu, Y., Brown, J. F., Verdin, J. P. and Wardlow, B.: A five-year analysis of MODIS NDVI and NDWI for grassland drought assessment over the central Great Plains of the United States, Geophys. Res. Lett., 34(6), doi:10.1029/2006GL029127, 2007.

Hall, J. V., Zhang, R., Schroeder, W., Huang, C. and Giglio, L.: Validation of GOES-16 ABI and MSG SEVIRI active fire products, Int. J. Appl. Earth Obs. Geoinformation, 83, 101928, doi:10.1016/j.jag.2019.101928, 2019.

Hanes, C. C., Wang, X., Jain, P., Parisien, M.-A., Little, J. M. and Flannigan, M. D.: Fire-regime changes in Canada over the last half century, Can. J. For. Res., 49(3), 256–269, doi:10.1139/cjfr-2018-0293, 2018.

Hanesiak, J. M., Stewart, R. E., Bonsal, B. R., Harder, P., Lawford, R., Aider, R., Amiro, B. D., Atallah, E., Barr, A. G., Black, T. A., Bullock, P., Brimelow, J. C., Brown, R., Carmichael, H., Derksen, C., Flanagan, L. B., Gachon, P., Greene, H., Gyakum, J., Henson, W., Hogg, E. H., Kochtubajda, B., Leighton, H., Lin, C., Luo, Y., McCaughey, J. H., Meinert, A., Shabbar, A., Snelgrove, K., Szeto, K., Trishchenko, A., Kamp, G. van der, Wang, S., Wen, L., Wheaton, E., Wielki, C., Yang, Y., Yirdaw, S. and Zha, T.: Characterization and Summary of the 1999–2005 Canadian Prairie Drought, Atmosphere-Ocean, 49(4), 421–452, doi:10.1080/07055900.2011.626757, 2011.

Hirsch, K. G., Corey, P. N. and Martell, D. L.: Using Expert Judgment to Model Initial Attack Fire Crew Effectiveness, For. Sci., 44(4), 539–549, doi:10.1093/forestscience/44.4.539, 1998.

Hobson, K. A., Bayne, E. M. and Wilgenburg, S. L. V.: Large-Scale Conversion of Forest to Agriculture in the Boreal Plains of Saskatchewan, Conserv. Biol., 16(6), 1530–1541, doi:10.1046/j.1523-1739.2002.01199.x, 2002.

https://doi.org/10.5194/nhess-2020-145
Preprint. Discussion started: 15 May 2020

Natural Hazards and Earth System Sciences Discussions

Hogg, E. H. (Ted): Climate and the southern limit of the western Canadian boreal forest, Can. J. For. Res., 24(9), 1835–1845, doi:10.1139/x94-237, 1994.

Johnston, J. M., Johnston, L. M., Wooster, M. J., Brookes, A., McFayden, C. and Cantin, A. S.: Satellite Detection Limitations of Sub-Canopy Smouldering Wildfires in the North American Boreal Forest, Fire, 1(2), 28, doi:10.3390/fire1020028, 2018.

Johnston, L. M. and Flannigan, M. D.: Mapping Canadian wildland fire interface areas, Int. J. Wildland Fire, 27(1), 1–14, doi:10.1071/WF16221, 2018.

Jolly, W. M., Nemani, R. and Running, S. W.: A generalized, bioclimatic index to predict foliar phenology in response to climate, Glob. Change Biol., 11(4), 619–632, doi:10.1111/j.1365-2486.2005.00930.x, 2005.

Kato, S., Kouyama, T., Nakamura, R., Matsunaga, T. and Fukuhara, T.: Simultaneous retrieval of temperature and area according to sub-pixel hotspots from nighttime Landsat 8 OLI data, Remote Sens. Environ., 204, 276–286, doi:10.1016/j.rse.2017.10.025, 2018.

Kidnie, S. and Wotton, B. M.: Characterisation of the fuel and fire environment in southern Ontario's tallgrass prairie, Int. J. Wildland Fire, 24(8), 1118–1128, doi:10.1071/WF14214, 2015.

Lee, B. S., Alexander, M. E., Hawkes, B. C., Lynham, T. J., Stocks, B. J. and Englefield, P.: Information systems in support of wildland fire management decision making in Canada, Comput. Electron. Agric., 37(1), 185–198, doi:10.1016/S0168-1699(02)00120-5, 2002.

Lewis, M., Christianson, A. and Spinks, M.: Return to Flame: Reasons for Burning in Lytton First Nation, British Columbia, J. For., 116(2), 143–150, doi:10.1093/jofore/fvx007, 2018.

Lieffers, V. J. and Stadt, K. J.: Growth of understory Piceaglauca, Calamagrostiscanadensis, and Epilobiumangustifolium in relation to overstory light transmission, Can. J. For. Res., 24(6), 1193–1198, doi:10.1139/x94-157, 1994.

Lieffers, V. J., Macdonald, S. E. and Hogg, E. H.: Ecology of and control strategies for Calamagrostiscanadensis in boreal forest sites, Can. J. For. Res., 23(10), 2070–2077, doi:10.1139/x93-258, 1993.

Lindley, T., Speheger, D. A., Day, M. A., Murdoch, G. P., Smith, B. R., Nauslar, N. J. and Daily, D. C.: Megafires on the Southern Great Plains, J. Oper. Meteorol., 7(12), 164–179, doi:10.15191/nwajom.2019.0712, 2019.

Lindley, T. T., Vitale, J. D., Burgett, W. S. and Beierle, M.-J.: Proximity Meteorological Observations for Wind-driven Grassland Wildfire Starts on the Southern High Plains, E-J. Sev. Storms Meteorol., 6(1) [online] Available from: https://ejssm.org/ojs/index.php/ejssm/article/view/67 (Accessed 4 December 2019), 2011.

McDowell, N. G. and Allen, C. D.: Darcy's law predicts widespread forest mortality under climate warming, Nat. Clim. Change, 5(7), 669–672, doi:10.1038/nclimate2641, 2015.

McGee, T., McFarlane, B. and Tymstra, C.: Chapter 3 - Wildfire: A Canadian Perspective, in Wildfire Hazards, Risks and Disasters, edited by J. F. Shroder and D. Paton, pp. 35–58, Elsevier, Oxford., 2015.

Parisien, M.-A., Walker, G. R., Little, J. M., Simpson, B. N., Wang, X. and Perrakis, D. D. B.: Considerations for modeling burn probability across landscapes with steep environmental gradients: an example from the Columbia Mountains, Canada, Nat. Hazards, 66(2), 439–462, doi:10.1007/s11069-012-0495-8, 2013.

https://doi.org/10.5194/nhess-2020-145
Preprint. Discussion started: 15 May 2020

Pickell, P. D., Coops, N. C., Ferster, C. J., Bater, C. W., Blouin, K. D., Flannigan, M. D. and Zhang, J.: An early warning system to forecast the close of the spring burning window from satellite-observed greenness, Sci. Rep., 7(1), 1–10, doi:10.1038/s41598-017-14730-0, 2017.

Reimer, J., Thompson, D. K. and Povak, N.: Measuring Initial Attack Suppression Effectiveness through Burn Probability, Fire, 2(4), 60, doi:10.3390/fire2040060, 2019.

Rogers, B. M., Soja, A. J., Goulden, M. L. and Randerson, J. T.: Influence of tree species on continental differences in boreal fires and climate feedbacks, Nat. Geosci., 8(3), 228–234, doi:10.1038/ngeo2352, 2015.

Sá, A. C. L., Benali, A., Fernandes, P. M., Pinto, R. M. S., Trigo, R. M., Salis, M., Russo, A., Jerez, S., Soares, P. M. M., Schroeder, W. and Pereira, J. M. C.: Evaluating fire growth simulations using satellite active fire data, Remote Sens. Environ., 190, 302–317, doi:10.1016/j.rse.2016.12.023, 2017.

Sanborn, P.: Topographically controlled grassland soils in the Boreal Cordillera ecozone, northwestern Canada, Can. J. Soil Sci., 90(1), 89–101, doi:10.4141/CJSS09048, 2010.

Schneider, R. R., Hamann, A., Farr, D., Wang, X. and Boutin, S.: Potential effects of climate change on ecosystem distribution in Alberta, Can. J. For. Res., 39(5), 1001–1010, doi:10.1139/X09-033, 2009.

Schneider, R. R., Devito, K., Kettridge, N. and Bayne, E.: Moving beyond bioclimatic envelope models: integrating upland forest and peatland processes to predict ecosystem transitions under climate change in the western Canadian boreal plain, Ecohydrology, 9(6), 899–908, doi:10.1002/eco.1707, 2016.

Srock, A. F., Charney, J. J., Potter, B. E. and Goodrick, S. L.: The Hot-Dry-Windy Index: A New Fire Weather Index, Atmosphere, 9(7), 279, doi:10.3390/atmos9070279, 2018.

Stockdale, C., Barber, Q., Saxena, A. and Parisien, M.-A.: Examining management scenarios to mitigate wildfire hazard to caribou conservation projects using burn probability modeling, J. Environ. Manage., 233, 238–248, doi:10.1016/j.jenvman.2018.12.035, 2019.

Stralberg, D., Wang, X., Parisien, M.-A., Robinne, F.-N., Sólymos, P., Mahon, C. L., Nielsen, S. E. and Bayne, E. M.: Wildfire-mediated vegetation change in boreal forests of Alberta, Canada, Ecosphere, 9(3), e02156, doi:10.1002/ecs2.2156, 2018.

Therneau, T., Atkinson, B., port, B. R. (producer of the initial R. and maintainer 1999-2017): rpart: Recursive Partitioning and Regression Trees. [online] Available from: https://CRAN.R-project.org/package=rpart (Accessed 15 December 2019), 2019.

Van Wagner, C. E.: Development and structure of the Canadian Forest Fire Weather Index System, Canadian Forestry Service, Ottawa. [online] Available from: https://cfs.nrcan.gc.ca/publications?id=19927 (Accessed 13 December 2019), 1987.

Whitman, E., Parisien, M.-A., Thompson, D. K., Hall, R. J., Skakun, R. S. and Flannigan, M. D.: Variability and drivers of burn severity in the northwestern Canadian boreal forest, Ecosphere, 9(2), doi:10.1002/ecs2.2128, 2018.

Whitman, E., Parisien, M.-A., Thompson, D. K. and Flannigan, M. D.: Short-interval wildfire and drought overwhelm boreal forest resilience, Sci. Rep., 9(1), 1–12, doi:10.1038/s41598-019-55036-7, 2019.

Wood, S.: mgcv: Mixed GAM Computation Vehicle with Automatic Smoothness Estimation. [online] Available from: https://CRAN.R-project.org/package=mgcv (Accessed 20 October 2019), 2019.

https://doi.org/10.5194/nhess-2020-145
Preprint. Discussion started: 15 May 2020

425 Zhang, T., Wooster, M. J. and Xu, W.: Approaches for synergistically exploiting VIIRS I- and M-Band data in regional active fire detection and FRP assessment: A demonstration with respect to agricultural residue burning in Eastern China, Remote Sens. Environ., 198, 407–424, doi:10.1016/j.rse.2017.06.028, 2017.

Zhang, T., Wooster, M. J., De Jong, M. C. and Xu, W.: How Well Does the 'Small Fire Boost' Methodology Used within the GFED4.1s Fire Emissions Database Represent the Timing, Location and Magnitude of Agricultural Burning?, Remote Sens., 430 10(6), 823, doi:10.3390/rs10060823, 2018.

Zoltai, S. C.: Southern limit of coniferous trees on the Canadian prairies, , 128 [online] Available from: https://cfs.nrcan.gc.ca/publications?id=12181 (Accessed 16 October 2019), 1975.

435

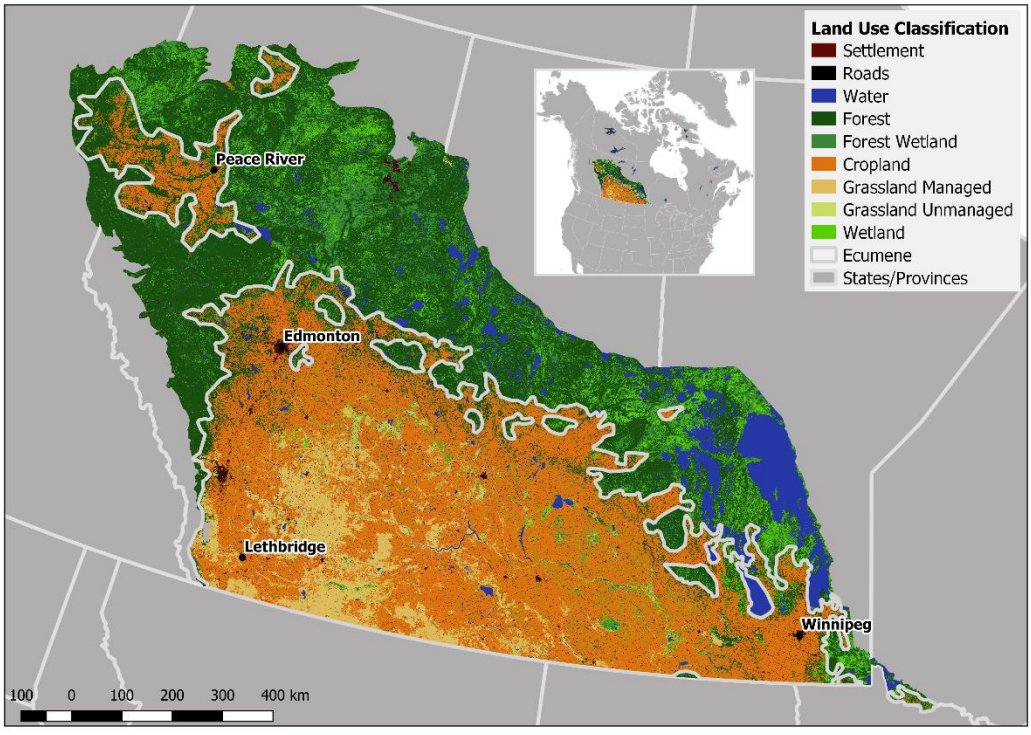

Figure 1. Landcover and study area extent.

https://doi.org/10.5194/nhess-2020-145
Preprint. Discussion started: 15 May 2020

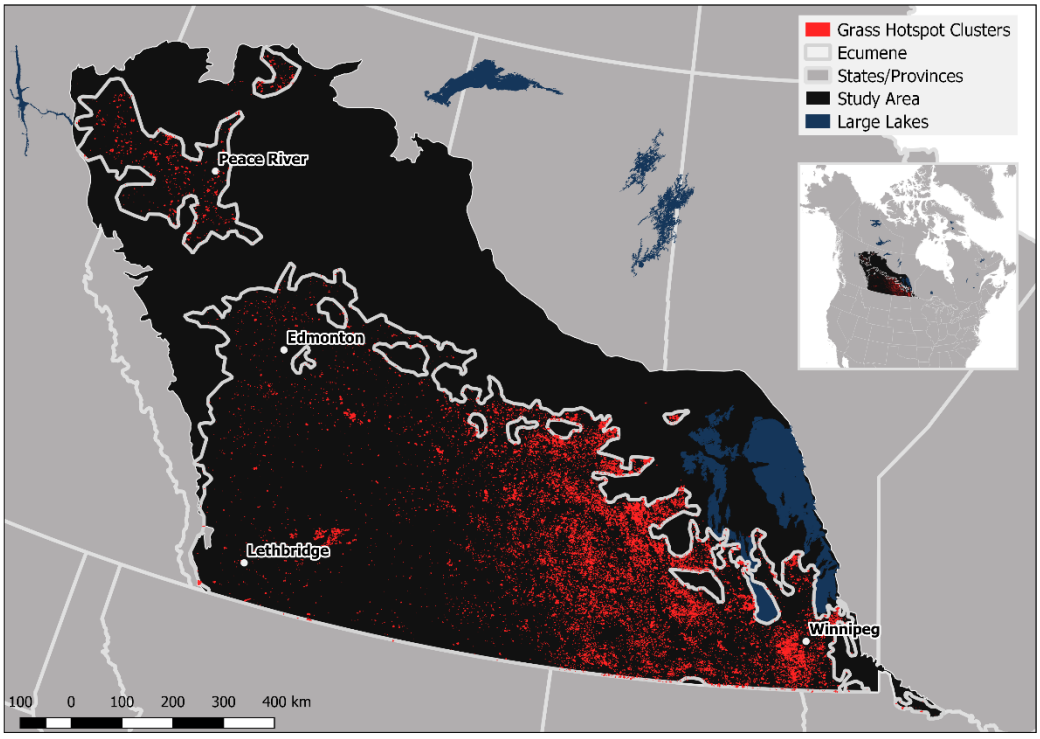

Figure 2: MODIS hotspots in the study area from 2002–2018.

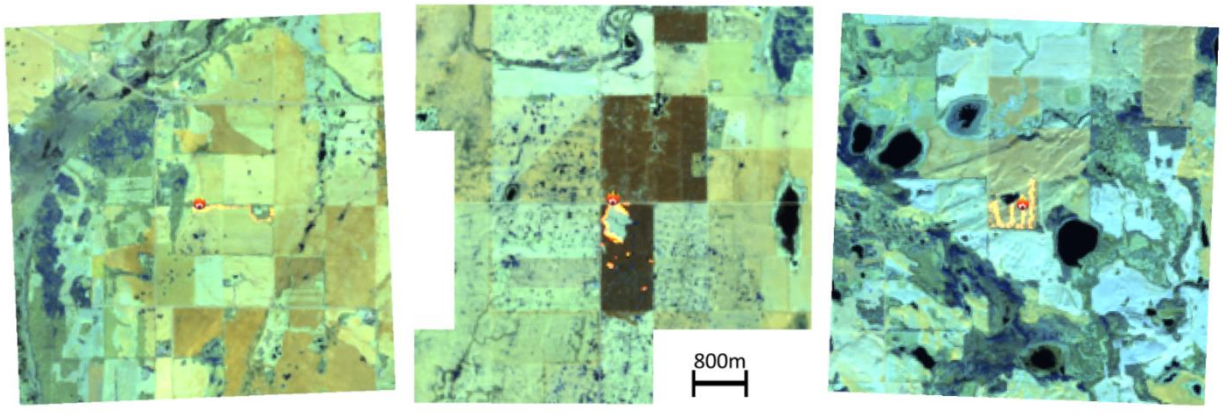

Figure 3. Examples of processed Landsat images indicating fire detections considered agriculture burns. Note the regular geometric patterns of the fires, specifically the line ignitions patterns and the burning of specific fields. The presence of previously burned fields is shown north of the active fire in the centre panel, which is registered in this study as low NDVI and very high rates of curing.

https://doi.org/10.5194/nhess-2020-145
Preprint. Discussion started: 15 May 2020

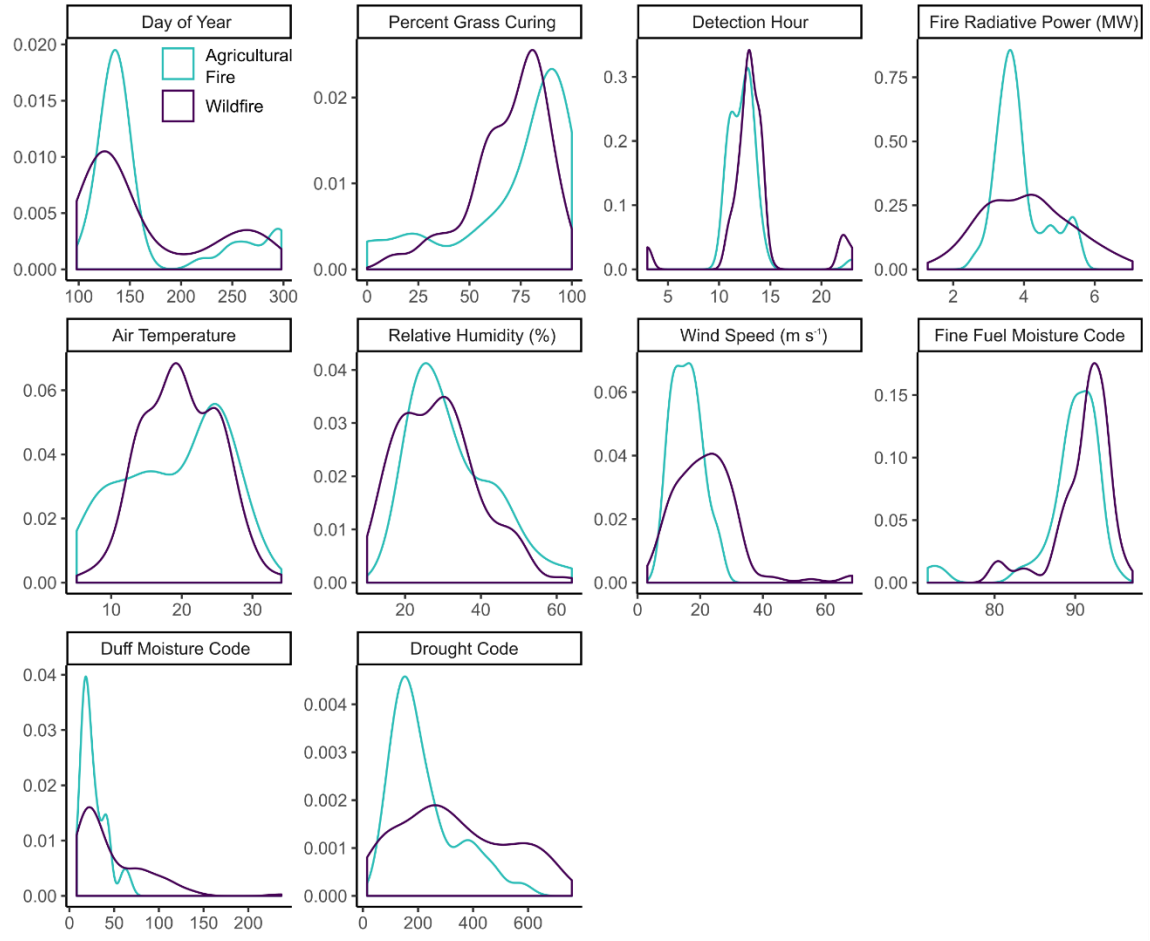

Figure 4: Distribution of fire detection properties between wildfires (purple) and agricultural fires (blue).

https://doi.org/10.5194/nhess-2020-145
Preprint. Discussion started: 15 May 2020

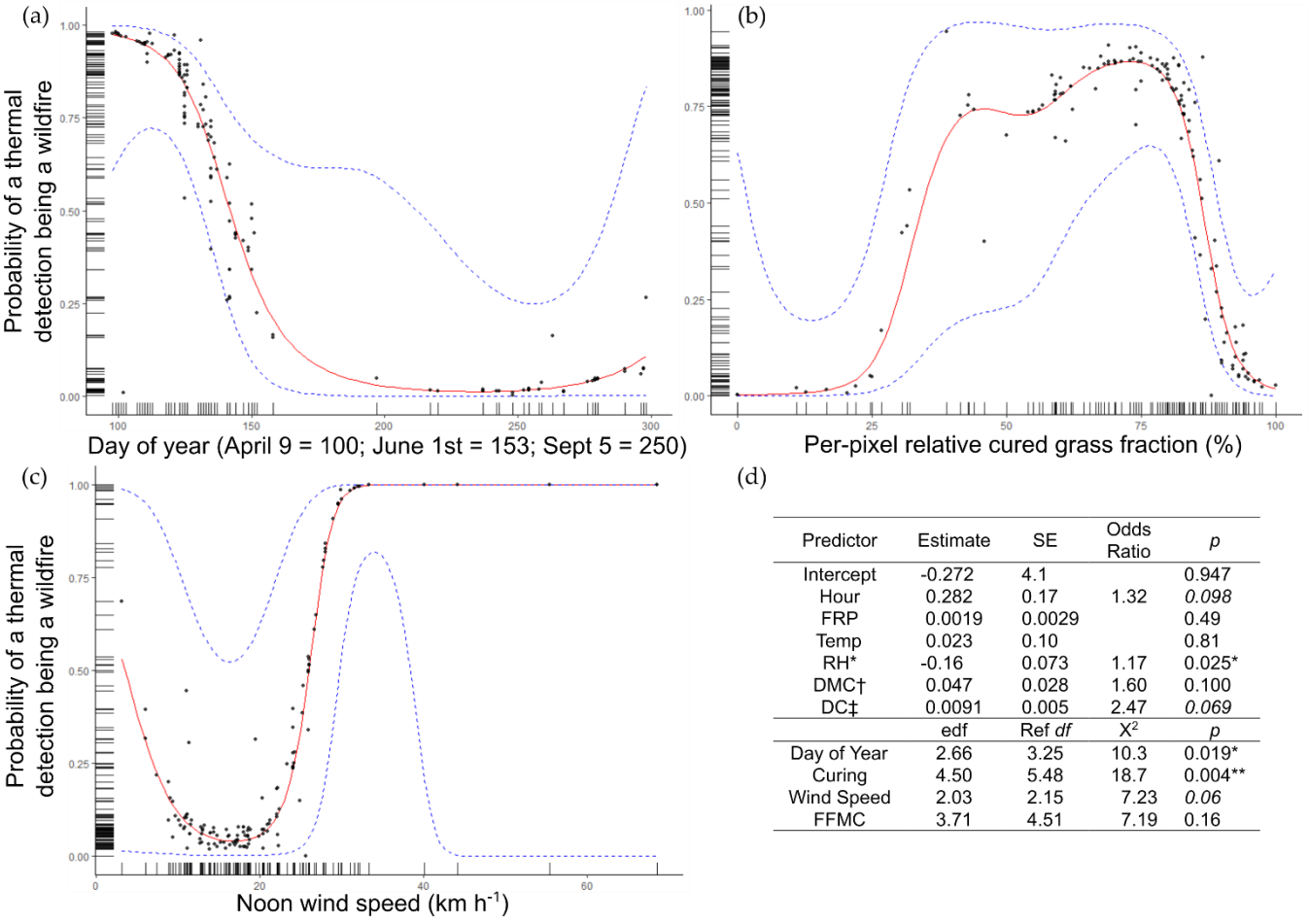

Predictor	Estimate	SE	Odds Ratio	*p*
Intercept	-0.272	4.1		0.947
Hour	0.282	0.17	1.32	*0.098*
FRP	0.0019	0.0029		0.49
Temp	0.023	0.10		0.81
RH*	-0.16	0.073	1.17	0.025*
DMC†	0.047	0.028	1.60	0.100
DC‡	0.0091	0.005	2.47	*0.069*
	edf	Ref *df*	X^2	*p*
Day of Year	2.66	3.25	10.3	0.019*
Curing	4.50	5.48	18.7	0.004**
Wind Speed	2.03	2.15	7.23	*0.06*
FFMC	3.71	4.51	7.19	0.16

Figure 5: Generalized Additive Model outputs for a binomial model of agricultural fire vs wildfire. The linear portions of the GAM coefficients (logit-transformed) are shown with Z values in panel (d), and the spline portions of the GAM are shown with X^2 (Chi-square) estimates in (d). Predictors significant at $p < 0.01$ are shown with **, $p < 0.05$ with *, and $0.1 > p > 0.05$ shown in italics. Logit-transformed parameter estimates of the GAM and Odds Ratios shown in panel (d). FRP = Fire Radiative Power; RH* = noon relative humidity, odds ratio shown as (estimate×−1), or odds ratio per unit decrease in RH; DMC† = Duff Moisture Code per 10 units; DC‡ = Drought Code per 100 units; FFMC = Fine Fuel Moisture Code.

https://doi.org/10.5194/nhess-2020-145
Preprint. Discussion started: 15 May 2020

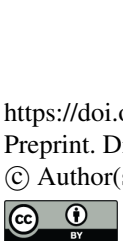

Natural Hazards and Earth System Sciences
Discussions

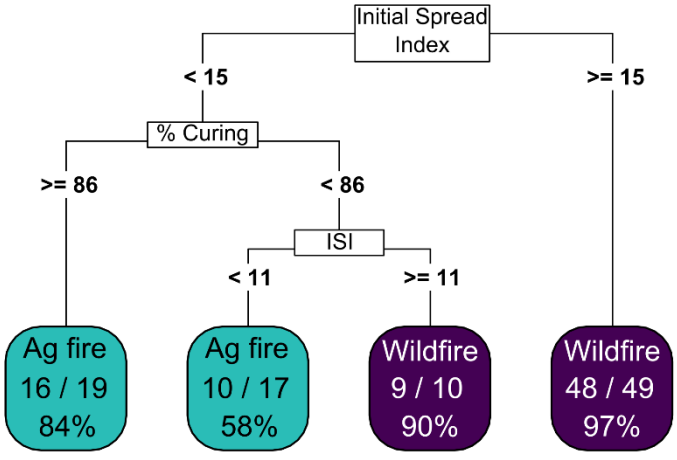

Figure 6. Simple decision tree scheme for the classification of agricultural vs wildfires, valid only for a subset of the dataset with Drought Codes exceeding 100. The first set of numbers in each terminal node is the number of correctly classified records divided by the total number of records in that node. The accuracy of each node is also given. Note that high rates of curing > 86% is associated with plowed fields or those previously burned in agricultural fires in the days prior (see Fig. 3).

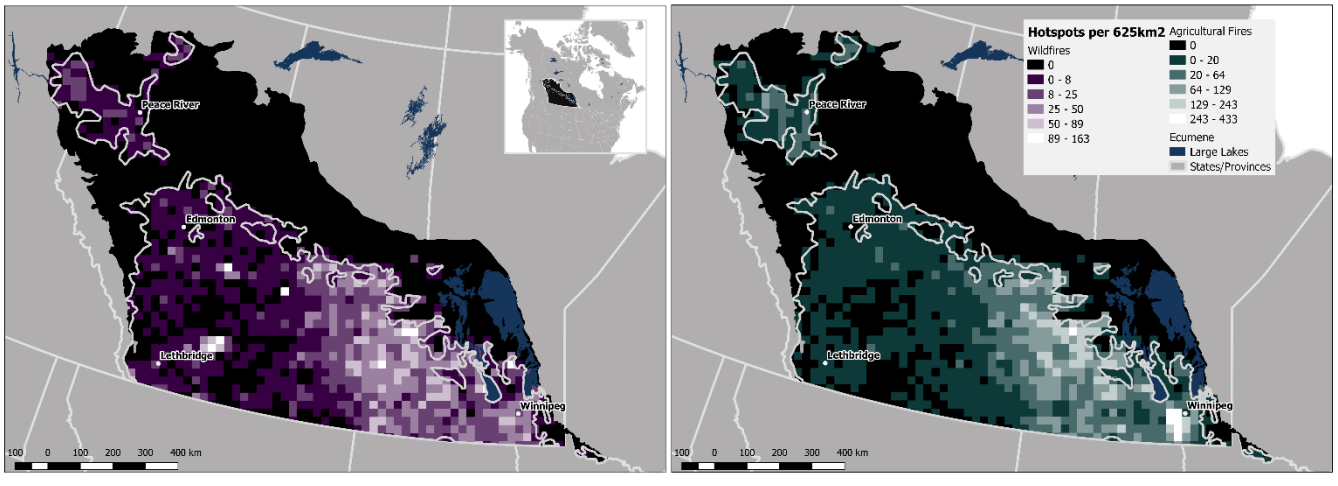

Figure 7. (a) Cumulative occurrence of wildfire hotspot detections r 625 km2 pixel) in the study region from 2002–2018. A wildfire may contain one or more hotspots. Panel (b) Cumulative occurrence of agricultural fire detections in the study region from 2002–2018.

https://doi.org/10.5194/nhess-2020-145
Preprint. Discussion started: 15 May 2020

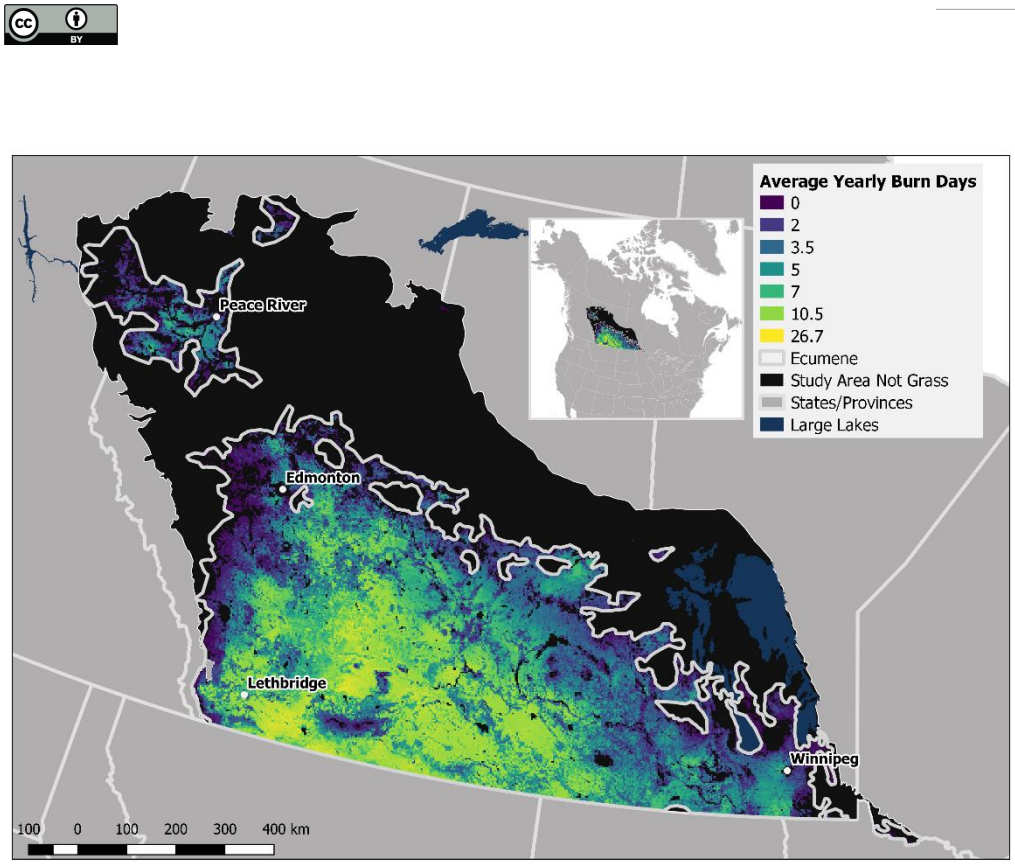

475 Figure 8. Average number of days per year (2002–2018) where the fire weather and environmental conditions meet or exceed the criteria in Fig. 6 for a grassland wildfire.

https://doi.org/10.5194/nhess-2020-145
Preprint. Discussion started: 15 May 2020

Natural Hazards and Earth System Sciences
Discussions

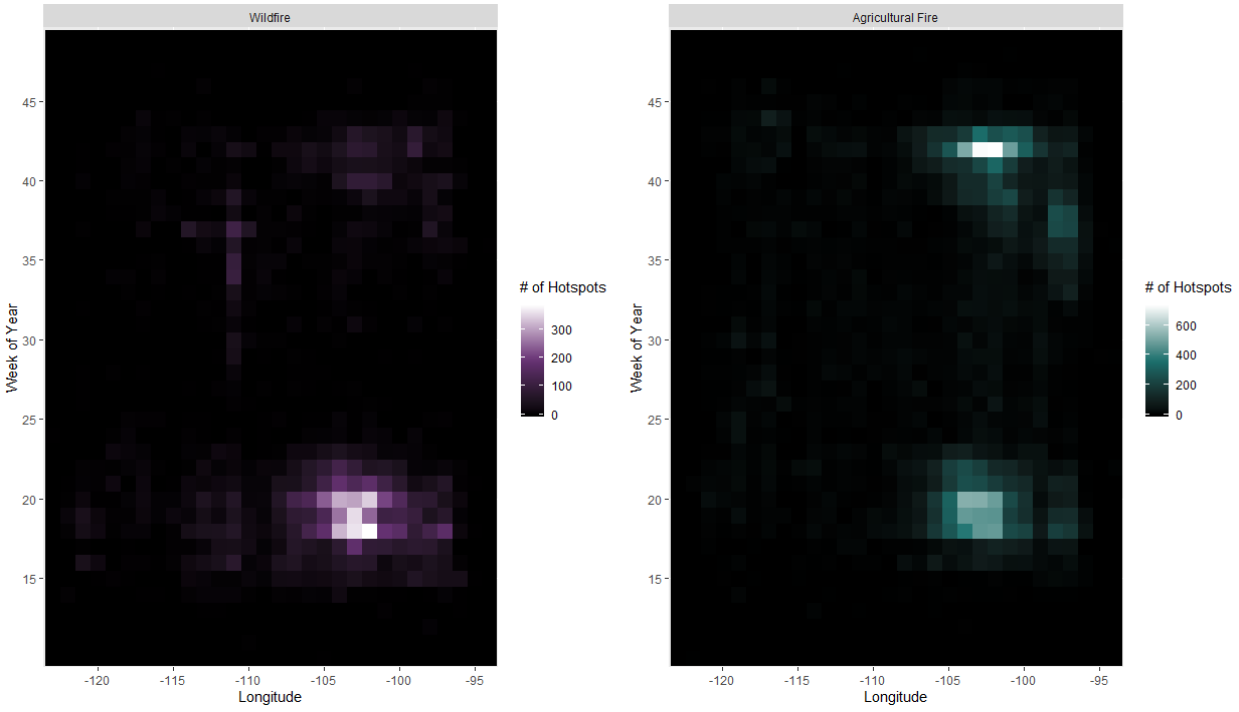

480 Figure 9. Hovmoller diagram showing seasonal patterns of wildfire vs agricultural fire. In this diagram, the number of hotspot detections is summed across all latitudes within a longitude bin (x-axis), and is shown over time (y-axis). Values are the cumulative sum of detections from 2002–2018.

Table 1. Generalized Additive Model (cutoff 0.70) and Decision Tree model performance metrics

Metric	GAM	Decision Tree
True Positive Rate - Sensitivity	0.82	0.98
True Negative Rate – Specificity	0.87	0.48
AUC	0.88	0.74
Miss Rate	0.17	0.01
False Positive Rate	0.12	0.51
False Discovery Rate	0.05	0.15
False Omission	0.32	0.09
Critical Success Index	0.78	0.82
Accuracy	0.84	0.85

485

https://doi.org/10.5194/nhess-2020-145
Preprint. Discussion started: 15 May 2020

Natural Hazards and Earth System Sciences
Discussions

Appendix A. Observation density biplots of the fire weather associated with thermal detections (n = 3036) where the Initial Spread Index of the Canadian Fire Weather Index System is 15 or higher (3036 of 24316 total observations, or 12%). Panel A: noon vapour pressure deficit vs wind speed (both local noon standard time) for all observations of ISI 15 or higher. Panel B: relative humidity vs wind speed for the same subset. Panel C: Fine Fuel Moisture Code vs wind speed.